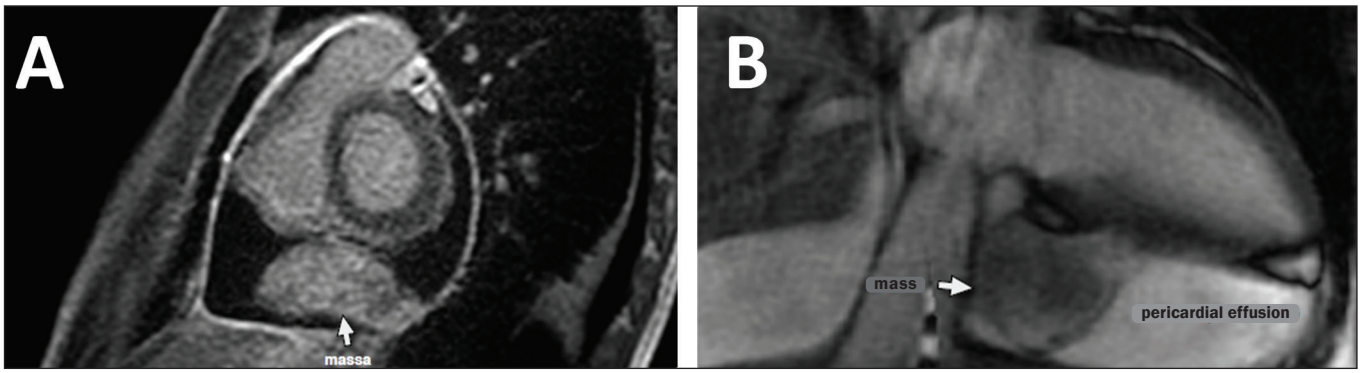

Figure 2. Cardiac MRI with delayed enhancement, in short-axis and long-axis views (**A** and **B**, respectively), showing a solid mass with a heterogeneous content, measuring 3.2 × 6.1 × 3.9 cm, in the posterior portion of the pericardial sac with adhesion points, with significant heterogeneous contrast uptake (as determined by the delayed enhancement technique), as well as pericardial inflammation.

surgical resection and radiotherapy, with or without chemotherapy[8,9]. In asymptomatic patients, the working diagnosis is based on incidental findings of lesions in cardiac imaging, whereas it is based on the findings of directed imaging tests in symptomatic patients; in either case, the diagnosis can be confirmed only through histopathological analysis[6,8].

Although the tumor image is nonspecific on the echocardiogram of an individual with pericardial synovial sarcoma, it is fundamental for the initial detection of the disease, quantification of the pericardial effusion, evaluation of cardiac function, and evaluation of cardiac restraint, as well as allowing comparative analysis with sequential follow-up examinations[10]. A solid, heterogeneous mass, with multilocular areas[11] and internal septa, is observed on CT and MRI; in some cases, there is invasion of adjacent structures, pericardial effusion and foci of metastases. Cardiac MRI is considered the best modality for the detection and characterization of pericardial synovial sarcoma, because it makes it possible to observe the degree of vascularization, to better detail the cardiac invasion, and to monitor the post-treatment evolution[10,12]. In this context, it can be concluded that, although the imaging tests do not confirm the diagnosis, they play a fundamental role in the detection and characterization, as well as in the preoperative and postoperative planning, of pericardial synovial sarcoma.

REFERENCES

1. Assunção FB, Oliveira DCL, Souza VF, et al. Cardiac magnetic resonance imaging and computed tomography in ischemic cardiomyopathy: an update. Radiol Bras. 2016;49:26–34.
2. Rochitte CE. Cardiac MRI and CT: the eyes to visualize coronary arterial disease and their effect on the prognosis explained by the Schrödinger's cat paradox. Radiol Bras. 2016;49(1):vii–viii.
3. Faistauer A, Torres FS, Faccin CS. Right aortic arch with aberrant left innominate artery arising from Kommerell's diverticulum. Radiol Bras. 2016;49:264–6.
4. Avelino MC, Miranda CLVM, Sousa CSM, et al. Free-floating thrombus in the aortic arch. Radiol Bras. 2017;50:406–7.
5. Bezerra SG, Brandão AA, Albuquerque DC, et al. Pericardial synovial sarcoma: case report and literature review. Arq Bras Cardiol. 2013;101: e103–e106.
6. Cheng Y, Sheng W, Zhou X, et al. Pericardial synovial sarcoma, a potential for misdiagnosis: clinicopathologic and molecular cytogenetic analysis of three cases with literature review. Am J Clin Pathol. 2012;137:142–9.
7. Chekrine T, Sahraoui S, Cherkaoui S, et al. Primary pericardial synovial sarcoma: a case report and literature review. JC Cases. 2014;9:40–3.
8. Salah S, Salem A. Primary synovial sarcomas of the mediastinum: a systematic review and pooled analysis of the published literature. ISRN Oncol. 2014;2014:412527.
9. Anand AK, Khanna A, Sinha SK, et al. Pericardial synovial sarcoma. Clin Oncol (R Coll Radiol). 2003;15:186–8.
10. Goldblatt J, Saxena P, McGiffin DC, et al. Pericardial synovial sarcoma: a rare clinical entity. J Card Surg. 2015;30:801–4.
11. Wu X, Chen R, Zhao B. Pericardial synovial sarcoma in a dyspnoeic female with tuberculous pericarditis: a case report. Oncol Lett. 2013;5:1973–5.
12. Restrepo CS, Vargas D, Ocazionez D, et al. Primary pericardial tumors. Radiographics. 2013;33:1613–30.

Diogo Costa Leandro de Oliveira[1], Eduardo Oliveira Pacheco[1], Larissa Teixeira Ramos Lopes[2], Claudio Calazan do Carmo[3], Alessandro Severo Alves de Melo[1]

1. Universidade Federal Fluminense (UFF), Niterói, RJ, Brazil. 2. Hospital Niterói D'Or, Niterói, RJ, Brazil. 3. Grupo Oncologia D'Or, Niterói, RJ, Brazil. Mailing address: Dr. Alessandro Severo Alves de Melo. Hospital Universitário Antonio Pedro. Rua Marques de Paraná, 303, 2° andar, Centro. Niterói, RJ, Brazil, 24033-900. E-mail: alesevero@gmail.com.

http://dx.doi.org/10.1590/0100-3984.2016.0200

Papillary tumor of the pineal region accompanied by Parinaud's syndrome: magnetic resonance imaging findings

Dear Editor,

A 22-year-old male patient presented with a nonpulsatile, diffuse headache of moderate-intensity, with no aura or other associated symptoms. In the neurological exam, he presented paralysis of the vertical conjugate gaze with fixed downward glance, bilateral eyelid retraction, insufficiency of ocular convergence, pupils nonreactive to light, and preserved pupillary reaction to accommodation, characterizing Parinaud's syndrome. Magnetic resonance imaging (MRI) showed an expansive lesion in the pineal region, with a discrete hyperintense signal in T1-weighted sequences and isointense in T2-weighted sequences, with cystic areas of diffusion, a discrete hyperintense signal in the diffusion, and marked gadolinium enhancement (Figure 1). The lesion caused compression of the cerebral aqueduct and dorsal midbrain, as well as causing hydrocephalus. Histopathological analysis demonstrated a papillary neoplasm composed of cuboidal cells, with an epithelial appearance, arranged on fibroconnective stromata, with evident vascularization, and mitotic activity (4 mitotic figures per 10 high-power fields). Immunohistochemical analysis showed marked positivity for cytokeratins and for S-100 protein, together with negativity for neurofilament proteins. These findings are consistent with a papillary tumor of the pineal region (PTPR).

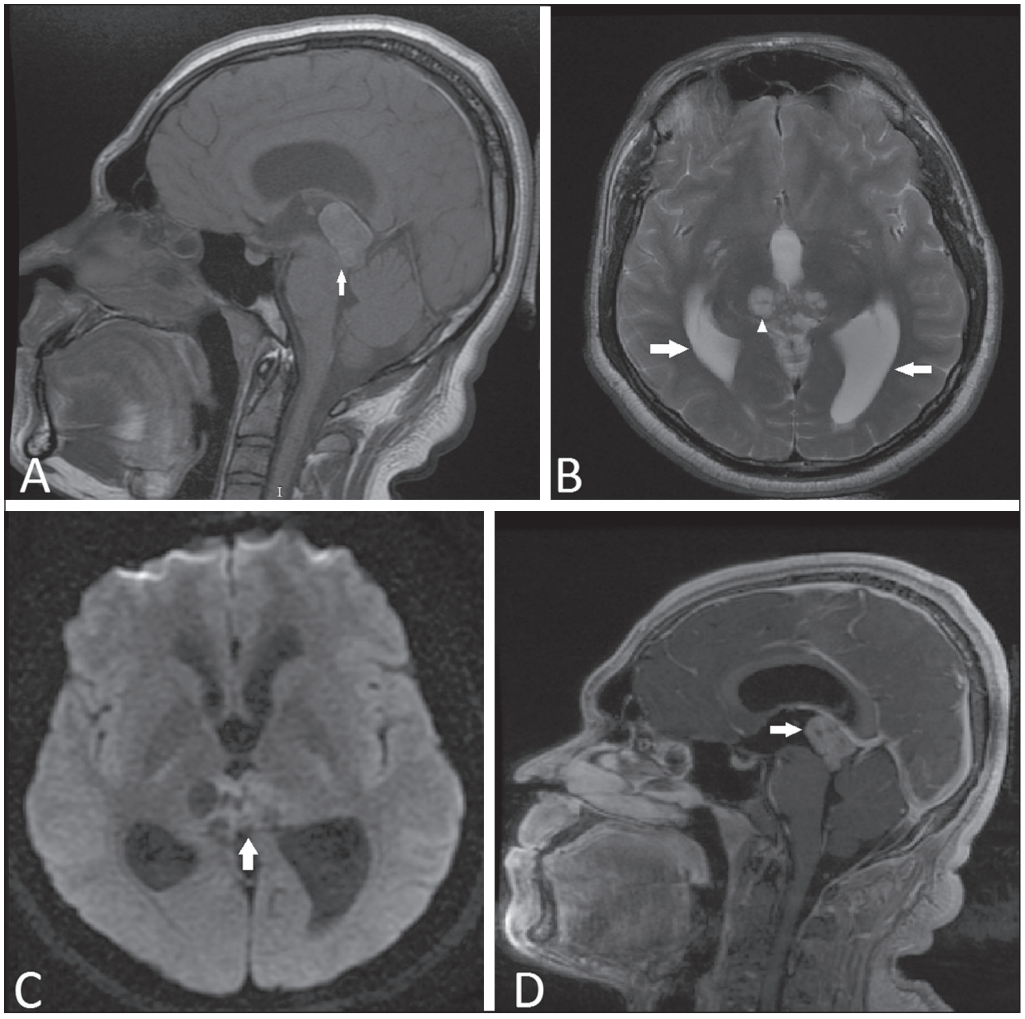

Figure 1. Magnetic resonance imaging. **A:** Non-contrast-enhanced sagittal T1-weighted sequence showing an expansile lesion in the pineal region compressing the dorsal midbrain and presenting a predominance of high signal intensity (arrow). **B:** Axial T2-weighted sequence showing cystic images within the lesion (arrowhead). Note also the increase in the dimensions of the supratentorial ventricular system (arrows). **C:** Functional diffusion-weighted sequence, axial section, showing discrete hyperintensity. **D:** Gadolinium contrast-enhanced sagittal T1-weighted sequence showing heterogeneous enhancement.

The role of MRI in the diagnosis of brain tumors has been expanding[1–3]. The World Health Organization classifies PTPR as a grade II or III tumor. It is rare, fewer than 200 cases having been reported. The mean age at onset is 35 years, and PTPR has no predilection for either gender[4]. Its origin is uncertain, the most widely accepted hypothesis is that it originates from ependymal cells of the subcommissural organ[4,5]. Histologically, PTPR is characterized by the presence of epithelial and papillary aspect structures with high cellularity and moderate-to-high mitotic activity[4–6]. It can cause headache, due to obstructive hydrocephalus, and Parinaud's syndrome[7], due to compression of the dorsal midbrain, specifically the periaqueductal region[8].

On MRI, PTPR typically presents as a heterogeneous, well-circumscribed mass in the pineal region, containing cystic areas, without calcifications or hemorrhages. Classically, it is described as showing a hyperintense signal in T1-weighted sequences, as observed in our case, the high signal intensity potentially being related to the high protein content of the lesion [9,10]. After intravenous administration of gadolinium, moderate heterogeneous enhancement is observed. Dissemination into the cerebrospinal fluid, although rare, occurs in up to 7% of cases[4,7]. Advanced MRI sequences can reveal signs of hypoperfusion, whereas proton spectroscopy can show increases in the peaks of choline, lactate, and myo-inositol, as well as a decrease in the N-acetyl-aspartate peak[11].

The differential diagnosis of lesions in the pineal region is broad, including germinoma, ependymoma, meningioma, pineocytoma, pineoblastoma, and glioma, although those tumors rarely present a hyperintense signal in T1-weighted sequences[10,11].

The treatment of choice is surgical resection, there being no proven benefits of the use of radiotherapy or chemotherapy[11]. Partial resection and tumors with higher mitotic and proliferative activity (high Ki-67 expression) tend to be related to a poor prognosis and to recurrence, which is reported in up to 72% of cases[4,11,12].

In conclusion, Parinaud's syndrome is a warning sign of the possibility of expansile processes in the pineal region. Albeit rare, the diagnosis of PTPR should be remembered among the hypotheses, especially when there is a hyperintense signal in a T1-weighted sequence.

REFERENCES

1. Queiroz RM, Abud LG, Abud TG, et al. Burkitt-like lymphoma of the brain mimicking an intraventricular colloid cyst. Radiol Bras. 2017;50:413–4.
2. Liaffa B, Noro F, Bahia PRV, et al. Dural fistula with bilateral arterial supply, mimicking a brainstem tumor. Radiol Bras. 2017;50:65–6.
3. Sharma R, Gupta P, Mahajan M, et al. Giant nontraumatic intradiploic arachnoid cyst in a young male. Radiol Bras. 2016;49:337–9.
4. Louis DN, Ohgaki H, Wiestler OD, et al. WHO classification of tumours of the central nervous system. 4th ed. Geneva, Switzerland: WHO Press; 2016. p. 180–2.
5. Kamamoto D, Sasaki H, Ohara K, et al. A case of papillary tumor of the pineal region with a long clinical history: molecular characterization and therapeutic consideration with review of the literature. Brain Tumor Pathol. 2016;33:271–5.

6. Jiménez-Heffernan JA, Bárcena C, Gordillo C, et al. Cytologic features of papillary tumor of the pineal region: a case report showing tigroid background. Diagn Cytopathol. 2016;44:1098–101.
7. Fauchon F, Hasselblatt M, Jouvet A, et al. Role of surgery, radiotherapy and chemotherapy in papillary tumors of the pineal region: a multicenter study. J Neurooncol. 2013;112:223–31.
8. Shields M, Sinkar S, Chan W, et al. Parinaud syndrome: a 25-year (1991-2016) review of 40 consecutive adult cases. Acta Ophthalmol. 2017;95:e792–e793.
9. Cerase A, Vallone IM, Di Pietro G, et al. Neuroradiological follow-up of the growth of papillary tumor of the pineal region: a case report. J Neurooncol. 2009;95:433–5.
10. Chang AH, Fuller GN, Debnam JM, et al. MR imaging of papillary tumor of the pineal region. AJNR Am J Neuroradiol. 2008;29:187–9.
11. Vaghela V, Radhakrishnan N, Radhakrishnan VV, et al. Advanced magnetic resonance imaging with histopathological correlation in papillary tumor of pineal region: report of a case and review of literature. Neurol India. 2010;58:928–32.
12. Fèvre-Montange M, Hasselblatt M, Figarella-Branger D, et al. Prognosis and histopathologic features in papillary tumors of the pineal region: a retrospective multicenter study of 31 cases. J Neuropathol Exp Neurol. 2006;65:1004–11.

Bruno Niemeyer de Freitas Ribeiro[1], Bernardo Carvalho Muniz[2], Nina Ventura[2], Emerson Leandro Gasparetto[2], Edson Marchiori[3]

1. Instituto Estadual do Cérebro Paulo Niemeyer and Universidade Federal do Rio de Janeiro (UFRJ), Rio de Janeiro, RJ, Brazil. 2. Instituto Estadual do Cérebro Paulo Niemeyer, Rio de Janeiro, RJ, Brazil. 3. Universidade Federal do Rio de Janeiro (UFRJ), Rio de Janeiro, RJ, Brazil. Mailing address: Dr. Bruno Niemeyer de Freitas Ribeiro. Instituto Estadual do Cérebro Paulo Niemeyer. Rua do Rezende, 156, Centro. Rio de Janeiro, RJ, Brazil, 20230-024. E-mail: bruno.niemeyer@hotmail.com.

http://dx.doi.org/10.1590/0100-3984.2016.0229

Inguinal and scrotal extramammary Paget's disease: ^{18}F-FDG PET/CT imaging

Dear Editor,

An 87-year-old man presented to our institution for investigation of an intertriginous rash, involving the left inner thigh, scrotum, and perineum, which had been neglected for a few years. The lesion was diagnosed as extramammary Paget's disease (EMPD). Due to the potential for EMPD to be associated with gastrointestinal and genitourinary malignancies, a thorough clinical and imaging evaluation was performed, the results of which were negative. The patient opted for symptomatic care only. Two years later, he returned to our institution with soft tissue swelling and edema of the left lower extremity, scrotum, and penis, with a nodular scrotal lesion and bilateral inguinal adenopathy (Figure 1). Positron emission tomography/computed tomography (PET/CT) showed ^{18}F-fluorodeoxyglucose (FDG)-avid lesions of the left scrotum, left inguinal lymph node, left pelvic lymph node, T12 vertebra, ribs, and left scapula (Figure 2). Biopsy of the left inguinal adenopathy showed signet-ring cells. Radiation therapy was initiated, resulting in partial improvement, followed by chemotherapy with carboplatin and paclitaxel. Unfortunately, the patient died, due to disease progression, at five months after the ^{18}F-FDG PET/CT imaging.

EMPD is a rare intraepithelial adenocarcinoma that typically gives rise to a pruritic rash at sites with numerous apocrine glands, such as the perineum, axilla, eyelids, scalp, and buttocks[1]. The disease occurs predominantly in patients over 50 years of age. In the Caucasian population, females are more affected than are males, whereas there is a predominance of males among EMPD patients in the Asian population[2]. The diagnosis of EMPD is based on the identification of Paget's cells with prominent nuclei and abundant lightly stained cytoplasm on hematoxylin-eosin staining[1,3]. The disease can arise from two major pathological mechanisms[4]: as an *in situ* intraepithelial adenocarcinoma which has the potential for local invasion and subsequent metastasis; and as pagetoid spread of a visceral

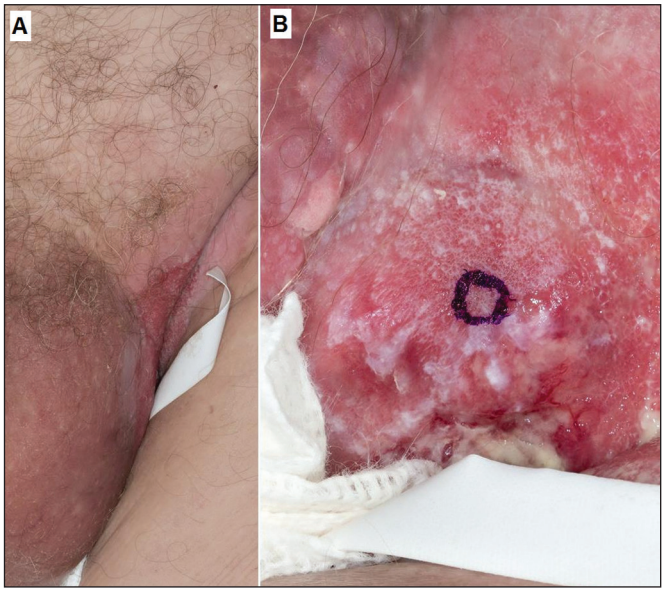

Figure 1. Photographs of a patient with EMPD. **A:** Lesions of the scrotum and left inguinal region. **B:** Close-up of the left inguinal lesion with a beefy red center and macerated whitish border.

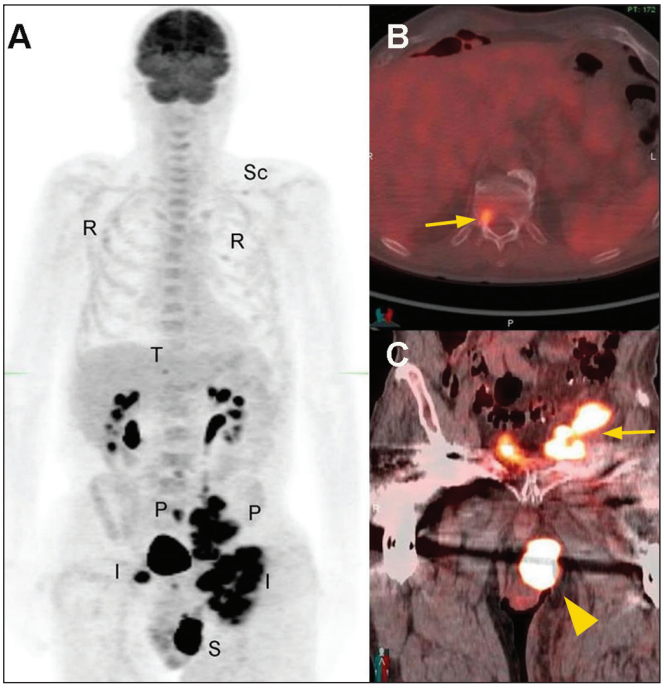

Figure 2. Maximum-intensity projection ^{18}F-FDG PET/CT (**A**) showing the left scrotal lesion (S), bilateral inguinal adenopathy (I), and pelvic adenopathy (P), as well as osseous metastases involving the T12 vertebra (T), multiple ribs (R), and the left scapula (Sc). Fused axial and coronal ^{18}F-FDG PET/CT images showing the T12 vertebra metastasis (arrow in **B**), together with the left scrotal lesion and left pelvic lymph node metastasis (arrowhead and arrow, respectively, in **C**).